GENERAL PAPERS

Organized by

A.M. Noce

Symposia Papers Presented Before the Division of Environmental Chemistry
American Chemical Society
Anaheim, CA March 28 – April 1, 2004

KINETIC MODELING OF OXIDATIVE COAGULATION FOR ARSENIC REMOVAL

Jin-Wook Kim and Timothy A. Kramer
Department of Civil Engineering, Texas A&M University,
250K WERC, College Station, TX 77843
waterkim@neo.tamu.edu, (Fax 979-862-1547)

INTRODUCTION

Of common oxidants, the application of Fenton's reagent may be successfully applied to conventional drinking water treatment processes. This success is especially true if, after the Fenton oxidation, the ferrous iron (Fe^{2+}) is converted to ferric iron (Fe^{3+}) such that the conventional coagulant, hydrous ferric oxide (HFO, am-$Fe(OH)_{3(s)}$, or 2-line ferrihydrite), is generated from ferric ion hydrolysis at a neutral pH range (6~8) and acts as both an arsenic adsorbent and suspended particle coagulant. The mass ratio of H_2O_2 to Fe^{2+} must be varied to find the optimum for oxidation. The hydrous ferric oxide formed will subsequently adsorb As(V) effectively. Thus, arsenic can be readily removed during the oxidative coagulation process consisting of oxidation, sorption and coagulation mechanisms.

RESULTS AND DISCUSSION

Arsenic Oxidation

A model of oxidative coagulation consisting of Fenton's reagent (Fe^{2+}/H_2O_2 at pH 7.0) was established and verified with experimental data (see Fig. 1). As shown in Fig. 1, an arsenic oxidation model using oxidative coagulation has high numerical accuracy at various pH ranges. Further, the oxidative coagulation model was extended to arsenic oxidation modeling at different initial conditions (reaction time of 30 min, $[As(III)]_o=0.5\times10^{-4}$ M, $[Fe^{2+}]_o=1.0\times10^{-3}$ M, $[H_2O_2]_o= 0.1\times10^{-3}$ ~1.0×10^{-3} M, pH 7.0, $[O_2]_{dissolved}$ = 2.5 M, HCO_3^- = 2.1×10^{-3} M) and is displayed in Fig. 2. The optimum condition was found when the mole ratio of As(III) : H_2O_2 : Fe^{2+} = 1 : 15 : 20. In this optimum condition, all of Fe^{2+} was converted to amorphous hydrous ferric oxide (am-$Fe(OH)_3$) and precipitated[1]. Thus, the hydrous ferric oxide generated from arsenic oxidation step can be used as an arsenic(V) adsorbent and particle coagulant.

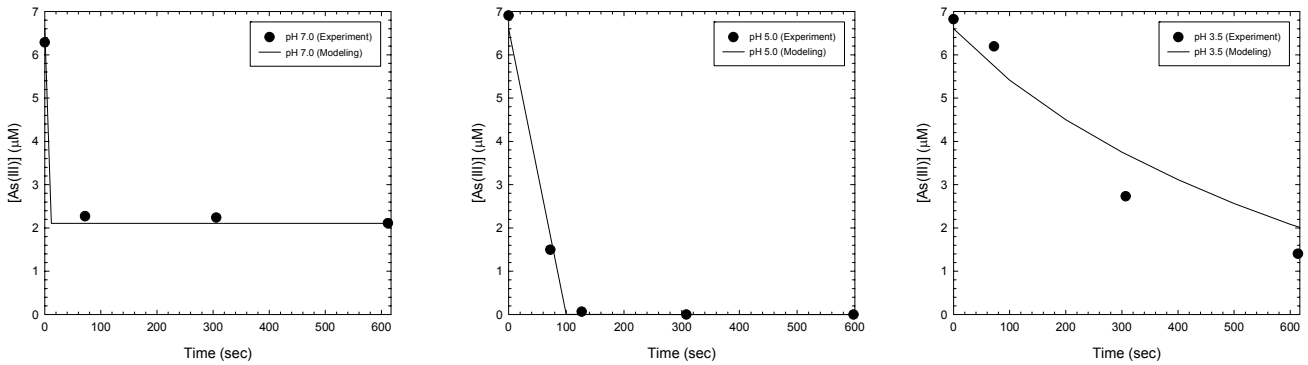

(a) (b) (c)

Figure 1. As(III) oxidation using oxidative coagulation at various pH conditions; (a) pH 7.0, (b) pH 5.0, (c) pH 3.5
([As(III)]$_o$=6.6μM, [Fe(II)]$_o$=20μM, [H_2O_2]$_o$=20μM) (Experimental data was adopted from Hug and Leupin[2]

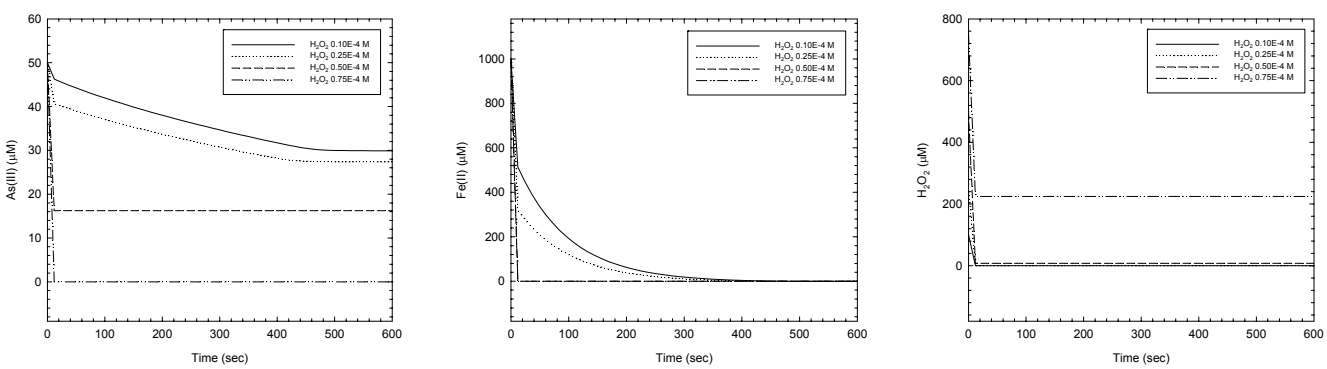

(a) (b) (c)

Figure 2. As(III) oxidation using oxidative coagulation at various H_2O_2 dose; (a) As(III), (b) Fe(II), (c) H_2O_2
([As(III)]$_o$=0.5×10^{-4} M, [Fe(II)]$_o$=1.0×10^{-3} M, [H_2O_2]$_o$= 0.1~1.0×10^{-3} M, pH 7.0, O_2 = 2.5 M, HCO_3^- = 2.1×10^{-3} M)

Arsenic Sorption

Two sorption models consisting of a chemical equilibrium model (surface complexation model) and a kinetic model (diffusion transport model) were developed. For chemical equilibrium modeling, PHREEQC[3] was introduced to couple the surface complexation model with sorption kinetic modeling. For arsenic sorption kinetic modeling, a diffusion transport model was developed to predict the arsenic sorption rate[4,5]. The results of surface complexation modeling were verified with experimental data at various

As(V)/HFO loading rates and displayed in Fig. 3. Prior to the sorption kinetic modeling, the Langmuir isotherm constants (q_o and b) by combining two As(V) being at different solid and liquid phases were determined using literature data[6]. The modeling results of the As(V) sorption kinetics were represented by Fig. 4(a) with respect to As(V) concentration and sorption capacity.

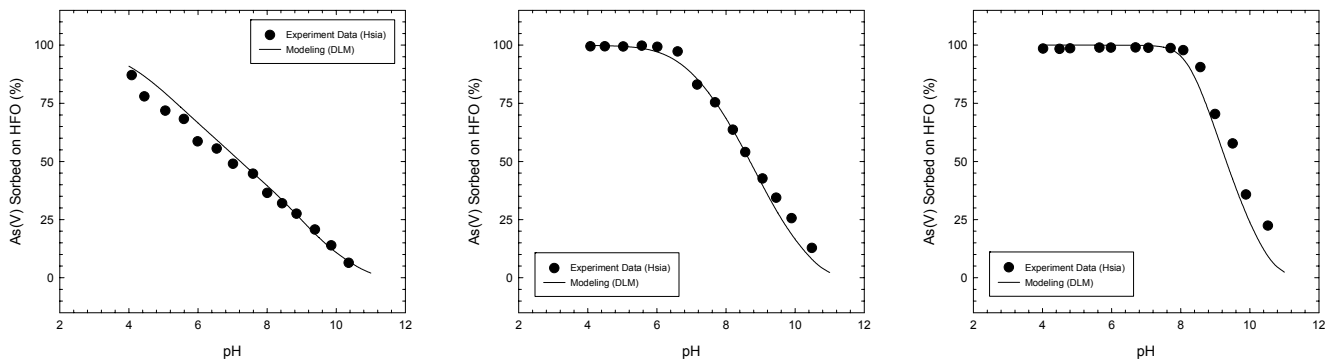

(a) (b) (c)

Figure 3. As(V) pH envelop at various arsenic(V) concentrations; (a) [As]=2.0×10^{-4} M, (b) [As]=1.0×10^{-4} M, (c) [As]=0.5×10^{-4} M ([Fe]=1.0E-3M, I=0.01M) (Experimental data was adopted from Hsia[7]

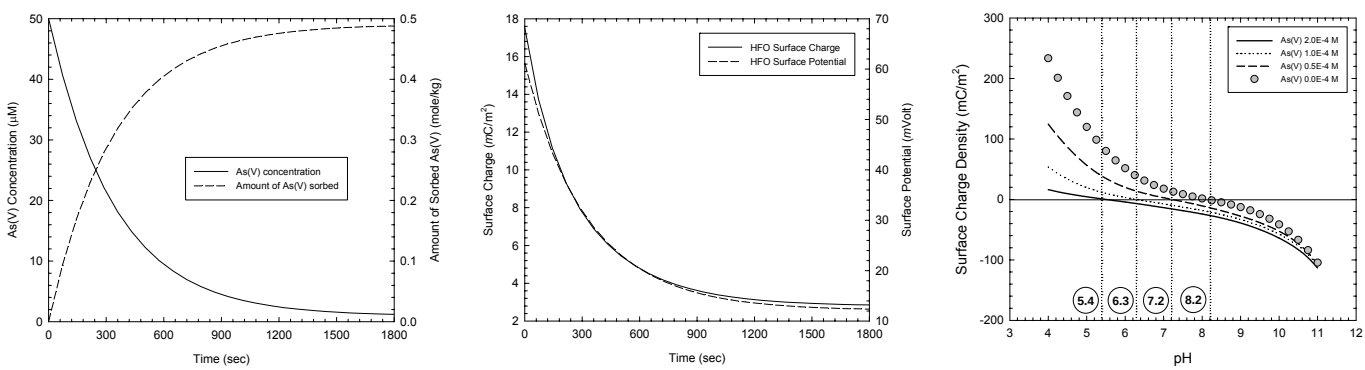

(a) (b) (c)

Figure 4. Kinetic modeling of As(V) sorption onto HFO and HFO surface charge evolution during As(V) sorption; (a) As(V) sorption kinetics, (b) surface charge kinetics, (c) pHzpc shift resulting from As(V) sorption ($[As(V)]_o$ = 0.5×10^{-4} M, HFO = 1.0×10^{-3} M as Fe, pH 7.0, I = 0.01 M)

Surface Charge/Potential Kinetics during Arsenic Sorption

To predict the kinetics of the HFO surface charge/potential during As(V) sorption, two sorption models (sorption kinetic model and surface complexation model) were coupled.

As a result, surface potential (ψ_d) kinetics during As(V) sorption could be calculated (see Fig. 4(b)) and the net surface energy (V_T) could be predicted and the surface energy kinetics is displayed in Fig. 5[8]. As shown in Figs. 4 and 5, the surface electrostatic repulsive energy (V_R) of HFO decreased in proportional to the amount of As(V) adsorbed onto the HFO. Further, the decreased electrostatic repulsive energy (V_R) lowered the net surface energy (V_T). That is, As(V) sorption onto HFO resulted in a lower energy barrier so that particle stability (W = 1 / collision efficiency) was decreased (increased particle collision efficiency).

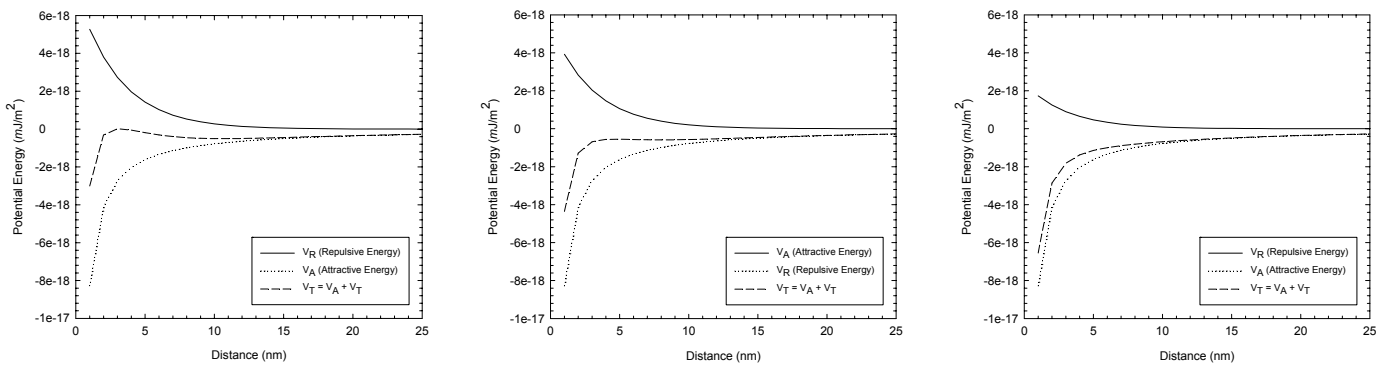

Figure 5. Surface energy evolution (total and repulsive energy) during As(V) sorption onto HFO; (a) 0 sec, (b) 72 sec, (c) 288 sec
($[As(V)]_o = 0.5\times10^{-4}$ M, HFO = 1.0×10^{-3} M as Fe, pH 7.0, I = 0.01 M)

Colloid Stability Kinetics

During arsenic sorption, the colloid stability (collision efficiency) kinetics resulting from the perikinetic coagulation mechanism (Brownian random motion) was calculated by considering inter-particle forces, van der Waals attractive force and electrostatic repulsive force, and displayed in Fig. 6[9-11]. As shown in Fig. 6, colloid surface potential was decreased from 60 mv to 12 mv in proportional to the amount of arsenic adsorbed onto HFO and this surface potential directly affected the colloid stability. When the surface potential is over 20 mv, colloid stability is very high so that colloid collisions are not expected (see Fig. 6(b)). By contrast, when the surface potential is less than 20 mv, colloid stability starts to decrease and colloid collisions can be expected. It was notable that at a surface potential of less 11.7 mv, collision efficiencies of 1.0 can be obtained. Thus, colloid aggregation initiated from arsenic sorption occurred in an elapsed time of 600 sec (surface potential less 20 mv). Further, after 1200 sec (surface potential 13 mv), colloid aggregation was extensive including a wide size range of aggregate particles.

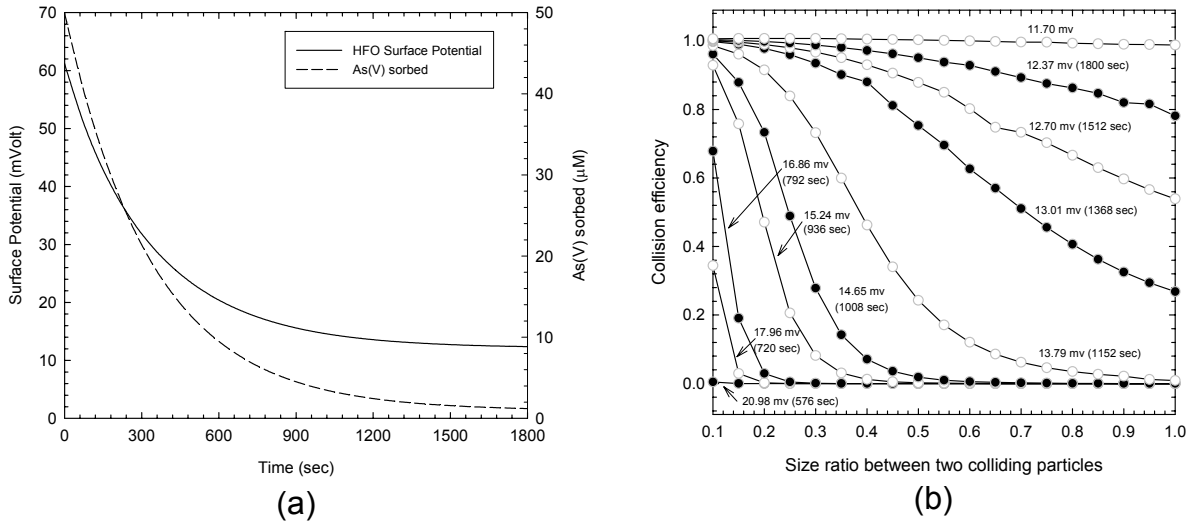

Figure 6. Collision efficiency between two colliding particles due to Brownian motion; (a) the kinetics of As(V) sorption and surface potential, and (b) collision efficiency at various surface potentials.

REFERENCES

1. Dzombak, D. A. and Morel, F. M. M., *Surface Complexation Modeling*, Wiley Interscience Publication, 1990.
2. Hug, S. J. and Leupin, O., *Environ. Sci. Technol.*, **37**, 2734, (2003).
3. Parkhurst, D. L. and Appelo, C. A. J., *User's Guide to PHREEQC(Version 2) - A Computer Program for Speciation, Batch-Reaction, One-Dimensional Transport, and Inverse Geochemical Calculations*, U.S. Department of the Interior and U.S. Geological Survey, Denver, CO., 1999.
4. Sparks, D. L., in *Soil Physical Chemistry*, D. L. Sparks, Ed., CRC Press, 1999, 135.
5. Fuller, C. C., Davis, J. A. and Waychunas, G. A., *Geochimica et Cosmochimica Acta*, **57**, 2271, (1993).
6. Pierce, M. L. and Moore, C. B., *Water Research*, **16**, 1247, (1982).
7. Hsia, T. H., Lo, S. L. and Lin, C. F., *Chemosphere*, **25**, 1825, (1992).
8. Stumm, W. and Morgan, J. J., *Aquatic Chemistry*, Wiley Interscience, 1996.
9. Valioulis, I. A. and List, E. J., *Adv. Colloid Interface Sci.*, **20**, 1, (1984).
10. Ho, N. F. H. and Higuchi, W. I., *J. Pharmaceutical Sci.*, **57**, 436, (1968).
11. Spielman, L. A., *J. Colloid Interface Sci.*, **33**, 562, (1970).